Noname manuscript No.
(will be inserted by the editor)

Co-optimization of Demand Response and Reserve Offers for a Price-Making Major Consumer

Mahbubeh Habibian · Golbon Zakeri · Anthony Downward · Miguel F. Anjos · Michael Ferris

the date of receipt and acceptance should be inserted later

Abstract We study demand-side participation in an electricity market for a large consumer of electricity, with some flexibility to reduce demand, and capable of offering interruptible load reserve. Our consumer is a price maker, and the impact of its actions in the market is modelled via a bi-level optimization problem. While the basic model for optimal consumption (only), has been laid out in [7, 14], our contribution consists of extending this model to the case where reserve offers need to be optimized simultaneously with consumption curves. Furthermore, we provide tailor made solution strategies for these problems under uncertainty, and report numerical results of our implementation on instances over the full New Zealand network yielding a realistic and large problem set.

Keywords Demand response · Bi-level optimization · Decomposition methods · Integer programming · Stochastic optimization

1 Introduction

Absence of demand response is considered an important market failure in electricity markets [8]. This absence prevents curtailment of demand in response to supply scarcity which is a necessity for any well functioning competitive market, particularly when power supply is unreliable. Electricity markets have started to enable consumers to be active participants, who can provide elasticity, and contribute to efficiency. Since the inception of disruptive technologies, (e.g. solar PVs and battery storage), there has been a growing body of work on household demand response [1, 16, 21, 24]. A number of authors have discussed demand response in restricted formats, e.g. [3, 4, 17] and have examined their potential and limitations [15,23]. However, there has been less research on full-scale models for large consumers of electricity with strategic bidding schemes.

Major users of electricity form an important group that can provide substantial demand response in any electricity market. In the US, approximately 30% of electricity is consumed by industrial consumers, while this figures is roughly 35% in New Zealand. In this paper, we model a price-maker consumer, who is capable of affecting the price of electricity through reduction of consumption. Our focus is on developing effective methodology for the solution of the resulting models to provide decision making tools, under uncertainty, for a large consumer of electricity in a realistic market setting. We report numerical results that demonstrate the effectiveness of our methodology. In a number of electricity markets (Singapore, Mid-continent ISO, New Zealand, etc), reserve and energy are co-optimized in the same market clearing auction. Such markets accept the traditional supply offers (offer stacks) and demand bids, furthermore they accept reserve supply offers (reserve stacks) that can be offered by generators or consumers capable of providing reserves. The reserves are typically fast responding reserves in the shape of tail water depressed (offered by hydro generators), or iterruptible load reserves (ILR) that is offered by major consumers. The capability of offering ILR offer stacks by the large consumer introduces another novel feature into

Address(es) of author(s) should be given

our work. Here, the major consumer not only decides on an optimal demand bid curve, but also simultaneously optimizes a reserve offer stack, both of which are submitted to the market. The stack nature of these curves provides some flexibility to cope with uncertainty, which is a cornerstone feature of our application given the make up of any electricity market, and volatility in prices.

In order to address the strategic bidding and offering of the major consumer, we present a bi-level optimization problem that maximizes the consumer's profit (the upper level problem), given the co-optimized optimal power flow problem (OPF) as the lower level problem. In this paper we focus on markets that operate as uniform price auctions with locational marginal pricing that co-optimize reserve and energy. We later lay out a comprehensive mathematical model of the co-optimized OPF in section 3. While a basic formulation of the stochastic bi-level program for optimal energy consumption of a large consumer in an electricity market has been offered in [7], no efficient methodology to solve this problem has been discovered prior to the current paper. Furthermore, we extend the model offered in [7], to include the optimal construction of a reserve offer stack in conjunction with optimizing the demand curve. This co-optimization makes the problem even more difficult to solve, and we develop tailor-made solutions that take advantage of our problem's structure. Our problem is important, as world wide, it leads to significant efficiency increases.

Similar models to ours have been introduced however our work is new and fundamentally different in several ways.

1. Our model allows for strategic interaction of the large consumer with the market in *both* demand response and reserve offers. Most papers to date (see e.g. [9,14]) either ignore the capability of the consumer to offer reserves, or assume the consumer to provide all reserves at price zero. We illustrate the importance of this feature of our model and the effects it has on the consumer's consumption strategy in subsection 2.1.
2. All existing literature uses the standard reformulations of complementarity conditions to MIPs. In contrast, we develop tailor made solution approaches for the resulting bilevel optimization problems that make it possible to solve these problems on a real electricity network consisting of several hundred nodes.
3. We offer a sampling methodology, from historical information, to make the solution procedure fully implementable for a large consumer and report on the results.

Our paper extends the work of Cleland et al. [5], to deliver admissible optimal policies in the form of a pair of demand curve and reserve stack (whereas the former paper only considers fixed consumption levels at any price). Secondly, we do not confine our solution to an apriori discretized set, rather, we optimize over the continuum of quantity and price. An example highlighting the differences of our work to the previous work is supplied in section 2.2.

We lay out the paper as follows. In section 2 we discuss the impacts of strategic co-optimization and the advantages of our proposed model in two illustrative examples. In section 2.2 we illustrate the extent of our contribution to the literature, with comparing our method with [5,6]. In section 3 we introduce the formulation of the NZEM market clearing problem in more detail, with discussion on the features of co-optimization. In section 4 we introduce our proposed bi-level formulation to capture the price-maker features of the major consumer. In section 4.1 we present standard and innovative alternate methods to reformulate our bi-level optimization problem. In section 5 we proceed to the stochastic version of our model. where the major consumer submits a monotone interruptible load reserve (ILR) offer curve and a demand bid curve. In section 6 we compare the solution times of the proposed decomposition method with the standard MIP reformulation and present our computational results for a large electricity consumer in the NZEM. Section 7 concludes the paper.

2 Price-Maker Major Consumer

Much of the literature on demand response has been from either a market design perspective, or from the point-of-view of industrial consumers who face exogenous prices. Recent changes to electricity markets have allowed for demand-side bids to be accepted into the spot market, enabling consumers to reflect their real-time elasticity to energy prices. Large consumers have sizable enough loads that reducing their consumption could have a palpable impact on the market prices. Due to the hockey stick nature of electricity stacks (as we approach system capacity the prices rise

sharply), responding to price in high peak periods not only reduces the purchase of high priced electricity but also leads to a decrease in spot prices. As an aside, this demand response can potentially reduce generation from expensive and polluting peaking plants. Our model considers a large consumer who takes account of the influence of their actions on the prices of energy (and reserve). This model allows the consumers to alleviate any pressure on reserve that may in turn affect the price of electricity . In this section we explore the characteristics of strategic behaviour for a major consumer. We first report on a sensitivity analysis of a strategic consumer's bid in a deterministic setting. This example is followed by the discussion on the impacts of strategic co-optimization on the consumer and the market. The second part of this section compares the method introduced in this paper with the most recent and relevant literature on co-optimized demand response in [6]. We will illustrate the difference of our methodology to existing methods.

2.1 Offering Reserve Matters

In this section we demonstrate that reserve offers make a significant difference to the optimal consumption strategy and ought not be left out of the decision making process. In what follows the generators and consumers are based at a single node. Although, a single-node market does not model the network effects, such as price differences between nodes, it still captures the effects that a major consumer has on the prices of energy and reserve. At this node we have 3 agents. A generator who is able to submit an energy offer stack and a reserve offer stack, inelastic demand (D), and our major consumer. We apply the turbine capacity constraints for the generators. Lastly, we set the major consumer as a strategic agent.

To show the impacts of co-optimization of electricity and reserve we construct two versions of this example. First we assume that the major consumer is only allowed to submit its quantity of consumption (y^d), but does not offer ILR; we call this version VS.1. In the second version the major consumer is able to offer a variable quantity of ILR (y^r), as well as deciding on the consumption quantity; we call this version, VS.2. To present a comprehensive illustration, we apply changes in inelastic demand at the node. We solve VS.1 and VS.2 for several levels of inelastic demand (from 65 to 130 MWh with steps of 1 MWh), and we plot the rendered optimal values.

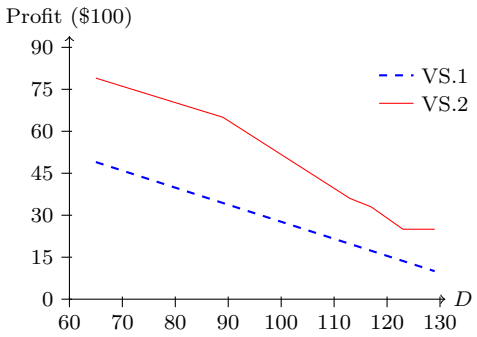

Fig. 1: Profit Maximizing Objective Function

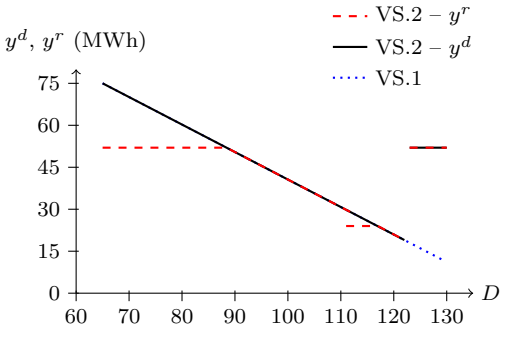

Fig. 2: Strategic Consumer Decision Variables

Fig. 1 demonstrates the optimal utility of the large consumer from VS.1 and VS.2 experiments. It shows that the consumer's optimal profit decrease as the in-elastic demand increases. Also, as anticipated, the results of this experiment show more profit in the co-optimized energy and reserve version, VS.2.

Next we report on the optimal values of y^d and y^r for the two experiments. Note that, as shown in Fig. 2, in VS.2, the ILR offer curve is always below the electricity consumption (dotted curve), indicating the consumer can not offer any more ILR (y^r) than the quantity consumed (y^d). The flat areas of ILR offer curve shows that, initially the consumer withholds from offering reserve at full capacity to utilize the higher prices of reserve. This pattern persists up to $D = 122$, where we observe a sudden increase in both electricity consumption and ILR offer. Although more consumption results in higher electricity prices, this cost is offset by being able to offer more ILR. On the other hand, in the absence of the option to supply ILR, in VS.1, the curve that corresponds

to y^d decreases constantly to keep the total demand (i.e. major consumer plus the inelastic demand) constant.

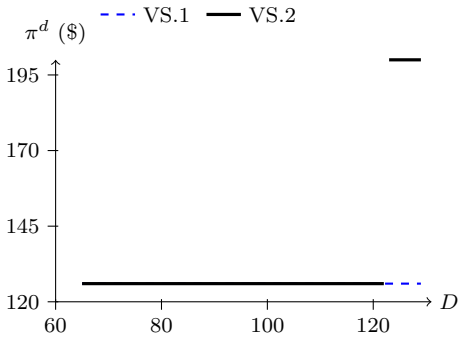

Fig. 3: Electricity Prices

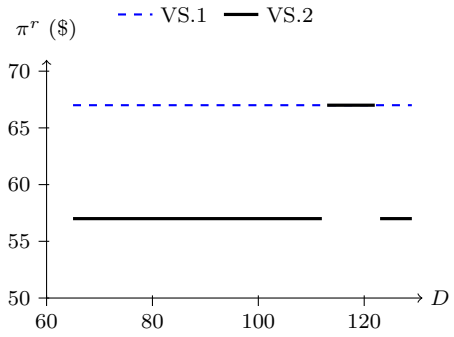

Fig. 4: Reserve Prices

The last set of results pertains to the clearing prices for energy π^d for the experiments (illustrated in Fig. 3) and reserve prices π^r, (illustrated in Fig. 4). We observe a jump in electricity price in VS.2, which is a result of sudden increase in electricity consumption. For the major consumer, this rise in electricity cost is compensated for by being paid more for ILR. In VS.1, the price is constant. The major consumer is able to keep the price constant, by decreasing its own demand to cancel out the increase in the inelastic demand.

Reserve price is also affected by ILR offers of the strategic agent. In VS.2, the reserve prices are at most equal to the VS.1 reserve prices. Note that in VS.2, reserve prices are more competitive with the participation of the major consumer in the reserve market. These results show that a major consumer who co-optimizes their energy bids and reserve offers strategically are able to improve their return.

2.2 Contrast to Previous Attempts

Models presented in several papers ([5, 9, 14]) look similar to our models at first glance. However [9, 14] essentially ignore the reserve complexity by assuming that the consumer is a price taker in that aspect. Furthermore the standard MPEC to MIP reformulations used in [9,14] do not solve our large scale and more complex problems. In [5, 6], Cleland et al. introduce a stochastic simulation based model(BOOMER-consumer) to solve the co-optimization of demand and reserve. They solve the problem of what *fixed* optimal quantity to consume and what is the optimal reserve stack coupled with this consumption quantity. In contrast, we address the real problem of offering the optimal *demand bid curve* and reserve offer to the market. To clarify these differences, we present an example based on a large consumer in the South Island of NZ, and compare our model to the Boomer-consumer method. Our sample space consists of 6 different scenarios from historical data of winter 2017. The aim is to produce optimal (in expectation) reserve stacks, while taking into account the co-optimization of reserve and energy in the NZEM. In order to make the optimal reserve stack, BOOMER fixes the consumption level and calculates the optimal reserve stack over the given scenarios for the given consumption level. For the sake of simplicity we limit our example to only 3 consumption levels. Table 2.2 shows the details of optimal solution values of reserve stacks for each consumption level as described in [5, 6].

Following the method used in BOOMER, we can construct the optimal reserve stack, given a fixed quantity of consumption. Figure 5 shows the reserve stacks that correspond to each designated fixed consumption level.

For comparison, we solve the same problem using our bi-level optimization model. The output of our model will be two stacks that maximize the expected profit. Table 2 presents the optimal solution values obtained from the bi-level method. Also, the corresponding monotone stacks are shown in Figures 6 and 7.

Table 1: BOOMER Optimal Reserve Stack Details

Consumption	400		600		700	
Scenario	Quantity	Price	Quantity	Price	Quantity	Price
a	0	0	0	0	0	0
b	2.362	0.5	5.049	0.5	37.997	0.5
c	2.362	6	5.049	6	67.652	0.5
d	22.643	43	28.642	74.1	67.652	15
e	2.362	42.1	24.365	15	67.652	0.5
f	2.362	15	5.049	15	67.652	0.5

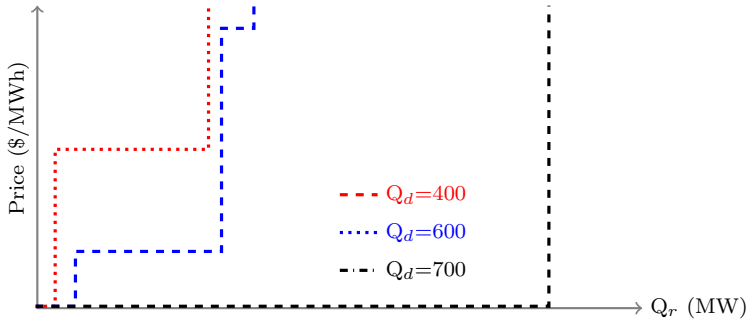

Fig. 5: Optimal wait-and-see reserve offers.

Table 2: Bi-level Optimal Stacks

Scenario	Electricity Quantity	Electricity Price	Reserve Quantity	Reserve Price
a	292.875	55	2.362	0
b	379.316	55	2.362	0.5
c	396.97	55	2.362	6
d	506.459	55	22.643	44
e	489.268	55	2.362	43.1
f	540.662	55	2.362	15

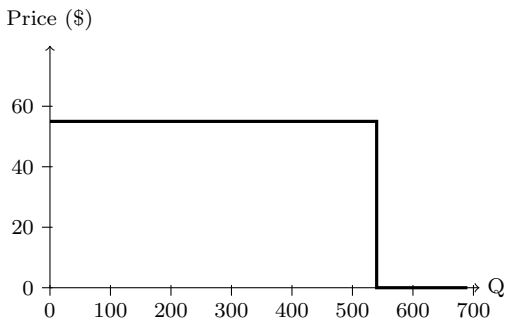

Fig. 6: Demand Bid

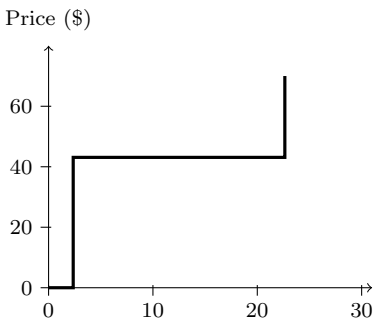

Fig. 7: Reserve Offer

The reserve stacks in the BOOMER method are better informed as they are tailored for a particular consumption level. However, the reserve offer shown in Figure 7 is optimized in expectation for various levels of consumption, which means it is a here and now decision rather than a wait and see approach. In order to complete this comparison we report on the difference in profit between the two methods in Table 2.2. Here, the bi-level method shows a better performance on average and in comparison with each of the designated consumption levels.

Table 3: Profit Comparison

Method	BOOMER			Bi-level
Consumption	400	600	700	
Expected Profit	12931.98	3826.73	-11493.8	15390.52

3 Co-optimized Optimal Power Flow Problem

In deregulated electricity markets, including the NZEM, a so called optimal power flow (OPF) market clearing problem is solved to determine the optimal dispatch of generation and locational marginal prices of electricity [22]. The optimal dispatch ensures that each of the North and South Islands have sufficient reserves procured against an $N-1$ contingency, where a large source of energy supply may trip (in either island). The NZEM employs two types of reserves. Fast instantaneous reserve (FIR), is a type of reserve that is available within six seconds of an unexpected generation or transmission outage. Sustained instantaneous reserve (SIR), is another type of reserve that is available within 60 seconds and must remain available for 15 minutes. Frequency keeping is partially co-optimized. In this paper the term reserve refers to FIR or SIR contingency reserve and not frequency keeping reserve. Additional examples of different terminology throughout the world is discussed in [10] and [11].

For the sake of simplicity and without loss of generality, in this section we lay out a single-node version of the co-optimized OPF that is solved in the NZEM, the full NZEM network's OPF problem is laid out in Appendix A. We use the following notation to formulate our model:

r	The required reserve level.
V	The minimum amount of difference between ILR and consumption. It denotes the level of consumption that can not be interrupted.
B	The fraction of generation allowed to be offered at reserve.
W	The maximum total amount of generation and reserve, offered by the generator.
$\mathcal{T'}_c$	The set of interruptible consumption tranches.
$\mathcal{Z}$	The set for types of tranches, i.e. consumption, generation, ILR and reserve. $\mathcal{Z} = \{c, g, rc, rg\}$
$\mathcal{T}_z$	The set of all offered tranches of type z.
x_t^z	The variable associated with the dispatch quantity tranche type z.
p_t^z	The price of tranche t of type z.
q_t^z	The quantity of tranche t of type z.
[ ]	Variables in [ ] indicate the duals of their associate constraints.

We denote this Linear Program (LP) as [D-LP]. generation ramp rate and capacity constraints are captured in [D-LP] as (3.5) and (3.6). These sets of additional constraints link the energy and reserve prices. Here x^{rg} is the procured reserve and x^g denotes the dispatched generation. Our ramp rate parameter is B, whereas R and W denote the maximum reserve offer and the unit capacity respectively. The constraints on generation and reserve ramp rate and capacity, form a so-called set of "inverse bathtub" constraints.

$$\text{[D-LP]} \max_{x^c, x^g} \sum_{t_c \in \mathcal{T}_c} p_{t_c}^c x_{t_c}^c - \sum_{t_g \in \mathcal{T}_g} p_{t_g}^g x_{t_g}^g - \sum_{t_{rg} \in \mathcal{T}_{rg}} p_{t_{rg}}^{rg} x_{t_{rg}}^{rg} - \sum_{t_{rc} \in \mathcal{T}_{rc}} p_{t_{rc}}^{rc} x_{t_{rc}}^{rc}$$

$$\text{s.t.} \quad \sum_{t_c \in \mathcal{T}_c} x_{t_c}^c = \sum_{t_g \in \mathcal{T}_g} x_{t_g}^g \qquad [\pi^d] \qquad (3.1)$$

$$- \sum_{z \in \{rc, rg\}} \sum_{t_z \in \mathcal{T}_z} x_{t_z}^z = -r \qquad [\pi^r] \qquad (3.2)$$

$$0 \le x_{t_z}^z \le q_{t_z}^z \qquad [\nu_{t_z}^{z+}, \nu_{t_z}^{z-}] \qquad (3.3)$$

$$\sum_{t_{rc} \in \mathcal{T}_{rc}} x_{t_{rc}}^{rc} - \sum_{t_c \in \mathcal{T'}_c} x_{t_c}^c \le 0 \qquad [\theta] \qquad (3.4)$$

$$\sum_{t_{rg} \in \mathcal{T}_{rg}^n} x_{t_{rg}}^{rg} \le B \sum_{t_g \in \mathcal{T}_g} x_{t_g}^g \qquad [\phi] \qquad (3.5)$$

$$\sum_{t_{rg}\in\mathcal{T}_{rg}} x^{rg}_{t_{rg}} + \sum_{t_g\in\mathcal{T}^n_g} x^g_{t_g} \le W \qquad [\phi']. \tag{3.6}$$

Here (3.3) holds $\forall t_z \in \mathcal{T}_z, \forall z \in \mathcal{Z}$. Note that (3.4) represents the constraint that ensures the large consumers' ILR level cannot be more than their curtailable load.

4 Bi-level Optimization

In order to capture the strategic behaviour discussed in section 2, we lay out a bi-level optimization problem, which has the OPF problem embedded inside. We start by assuming that this consumer maximizes its utility by consuming a fixed quantity (y^d), and offering a fixed quantity (y^r) for ILR. Here, the electricity market clearing problem [D-LP] is embedded within the price maker consumer's profit optimization problem, rendering a leader-follower type model captured as a bi-level program.

For the sake of simplicity, we lay out a Bi-level problem that is solved over a single-node market, and the bi-level optimization model for the multi-node network is presented in Appendix A. In addition, we define the utility function for consumption of electricity $\mathcal{U}(y^d) = uy^d$ where u is a constant. However the results are applicable for any concave utility/costs function $\mathcal{U}(y^d)$. The objective is to maximize the profit, taking into account revenues obtained through ILR. The cost of offering ILR only affects the major consumers if they are actually called upon to interrupt their load. We define the probability of being called upon to be ρ^r. Hence, the utility part of our objective function is: $u(y^d - \rho^r y^r)$, where in practice $\rho^r \simeq 0$. For the sake of simplicity (and generally without any effect on the optimal solution), we omit $\rho^r y^r$ from the objective function. We lay out the bi-level optimization problem, that we call [B-L], below:

$$\begin{aligned}
[\text{B-L}] \quad & \max_{y^d, y^r} \quad uy^d - \pi^d y^d + \pi^r y^r \\
& \text{s.t.} \quad 0 \le y^d \le C^d && (4.1)\\
& \qquad 0 \le y^r \le C^r && (4.2)\\
& \qquad y^d - y^r \ge V && (4.3)\\
[\text{D-LP2}] \quad & \max_{x^{z|z\in\mathcal{Z}}} \sum_{t_c\in\mathcal{T}_c} p^c_{t_c} x^c_{t_c} - \sum_{t_g\in\mathcal{T}_g} p^g_{t_g} x^g_{t_g} - \sum_{t_{rg}\in\mathcal{T}_{rg}} p^{rg}_{t_{rg}} x^{rg}_{t_{rg}} - \sum_{t_{rc}\in\mathcal{T}_{rc}} p^{rc}_{t_{rc}} x^{rc}_{t_{rc}} \\
& \text{s.t.} \quad (\textbf{??}) - (3.6) \\
& \qquad \sum_{t_c\in\mathcal{T}_c} x^c_{t_c} = \sum_{t_g\in\mathcal{T}_g} x^g_{t_g} - y^d \qquad [\pi^d] && (4.4)\\
& \qquad - \sum_{t_z\in\mathcal{T}^n_z} x^z_{t_z} = y^r - r_e \qquad [\pi^r]. && (4.5)
\end{aligned}$$

Note that the consumer also has a limit on their ILR offer constituted by their level of consumption and a load margin V that can not be interrupted. We call the market clearing problem in this model [D-LP2]. The difference between this problem and the previous version ([D-LP]) is adding the upper level variables y^d and y^r in (4.4) and (4.5) as inelastic demand and ILR for the lower level problem; this is equivalent to being offered at infinite and zero price respectively, to insure full dispatch. These two sets of variables are deemed to be constants in the primary dispatch model [D-LP2]. A common approach to solve a bi-level problem is through reformulating it into an MPEC, by replacing the lower level problem with its optimality conditions. However, most standard MPEC solvers will not guarantee global optimality due to non-convexities arising from the optimality conditions of the lower level problem. Therefore, to find a global optimum, we reformulate [B-L] as a MIP. Following [13] and [12] we use the KKT conditions of the dispatch problem, and binary variables with big-M right-hand sides to enforce the complementary constraints. This technique is used in [20] and [19] to convert a profit maximizing bi-level optimization problem for generators to a MIP. In [2], binary expansion is used to reformulate the day-ahead market MPEC problem to a MIP, but the approach did not scale for the examples over several agents. In addition to the complexity of solving the MIP over a large network , our model must also capture the co-optimization of energy and reserve. In our MIP, reserve and electricity prices are linked by the

constraints (3.4)-(3.6). Although this reformulation will enable us to get the global optimum, the nature of integer optimization impedes efficient solution times as the problem becomes larger with the introduction of uncertainty. In section 4.1 we introduce a novel reformulation method to solve [B-L], and compare it with the performance of the standard MIP reformulation in section 6, in a case study.

4.1 Bi-variant Sensitivity Analysis Reformulation Method

In this section, we introduce a reformulation method to solve [B-L], using a bi-variant sensitivity analysis algorithm. The idea is to explicitly capture reserve and energy prices at a node n, as functions of the actions of the strategic consumer who is located at n, using the fundamentals of the simplex method[1]. In practice, the bi-level problem is solved over a large electricity market, which may operated over a large network. For instance, the NZEM consists of around 300 nodes, but the only nodal prices that affect our decisions are those corresponding to the strategic consumer's node. If we can find the energy and reserve prices as a function of the consumer's actions $(\pi_d, \pi_r) = f(y^d, y^r)$, each scenario could be reduced to a point-to-set mapping for price, instead of modelling all the details of the dispatch problem, that resulted in the complex [MIP] problem.

In this method we use sensitivity analysis on the right-hand sides of the two constraints that determine the nodal energy and reserve prices in the lower level problem for the major consumer. In [B-L], these two constraints are (A.12) and (A.13). By employing an iterative algorithm, we define regions corresponding to bases of the lower level optimization problem [D-LP2]. For each basis, there exists a pair of prices (π^d, pi^r) which are constant with respect to right hands terms (y^d, y^r) while that basis is optimal. In Appendix B, we lay out the algorithm for reformulating a generic LP via using our bi-variant sensitivity analysis method.

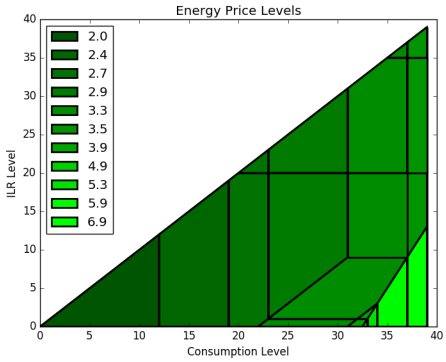

Fig. 8: Energy Price Regions

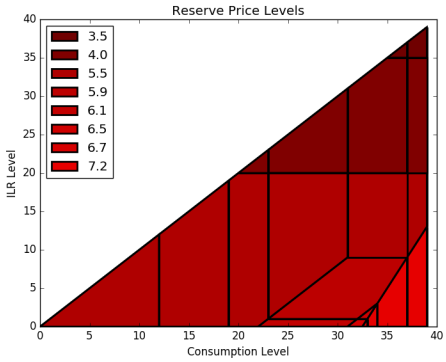

Fig. 9: Reserve Price Regions

Figures 8 and 9 demonstrate the decomposed regions, defined by the vertices obtained through our bi-variant sensitivity analysis, for a 4-node network. Here regions are divided by black lines, with a top down view. Here, each demonstrated region has a unique corresponding reserve and energy price. However, when we have a degenerate solution at the edge of one region, the price of energy or reserve could be a convex combination of prices in the two adjacent regions. In order to address this, we have assigned "vertical regions" to the edgers of regions, more detail on this is presented in Appendix B .

In Fig. 8 each shade correspond to a region that price of energy is constant. Similarly, Fig. 9 presents the regions that price of reserve is constant (denoted by regions of red). As shown in these regions, the price of energy and reserve increase as the level of consumption goes up, and the reserve price decreases as the consumer offers more ILR.

[1] In this method, we only allow for strategic consumers who purchase electricity and offer ILR at just one node. Our algorithm may not be applicable for consumers that are located at multiple nodes

This reformulation method simplifies the lower level problem, while keeping the exact information regarding the interactions of strategic consumer's consumption of ILR with the market. For instance, Figures 8 and 9 show the effect of offering ILR, when the other generators in the market are at their maximum capacity. The tilted lines represent that a generators in this network has a binding inverse bathtub constraint.

5 Stochastic Demand Response

In section 4, we assumed full information about the electricity market, including information on bids and offers of other market participants. While a deterministic model is a useful starting point, in reality we are exposed to uncertainty and lack of information about the market data. Furthermore, the bidding mechanism into the market, requires consumption and reserve offer stack. To address these, we will develop a stochastic version of our model, where the consumer faces a set of scenarios $\omega \in \Omega$ with probability ρ_ω for scenario ω. These scenarios can capture different levels of system demand for instance, or different generation offers. We can model this stochastic optimization problem with solving the standard [MIP] model (which was described in section 4) over the set Ω, and obtain the optimal expected profit, and denote it [S-MIP]. However, solving [S-MIP] for a full-scale model restrict us to few number of scenarios.

In order to reduce complexity of this stochastic model, we employ the bi-variant sensitivity analysis reformulation and calculate the regions corresponding to the dispatch problem of each scenario. Subsequently, we lay out a mixed integer program (presented as [α-MIP]) that reads in the regions corresponding to each scenario $\omega \quad (\forall \omega \in \Omega)$ and outputs the optimal expected reserve and energy stacks over Ω, given the objective of profit maximization for the major consumer. Assume that R^ω is the set of all regions retrieved from the algorithm described in 4.1, for scenario ω, and R_i^ω as the set of all the extreme points that form region i in R^ω. In this model, the points within region i is designated by 4 values, and we note $\hat{y}_{i,j}^{d^\omega}$ as the consumption level of the extreme point j of the region i in set $\mathcal{R}^\omega$. Similarly, we note the corresponding reserve level, energy and reserve prices, by $\hat{y}_{i,j}^{r^\omega}$, $\hat{\pi}_{i,j}^{d^\omega}$ and $\hat{\pi}_{i,j}^{d^\omega}$ respectively.

$$
\begin{aligned}
[\alpha\text{-MIP}] \quad \max_{y^d, y^r} \quad & \sum_{\omega \in \Omega} \left(u * y^{d^\omega} - \psi^{d^\omega} + \psi^{r\omega} \right) \\
\text{s.t.} \quad & \psi^{d^\omega} = \sum_{i \in \mathcal{R}^\omega} \sum_{j \in \mathcal{R}_i^\omega} \alpha_{i,j}^\omega \hat{y}_{i,j}^{d^\omega} \hat{\pi}_{i,j}^{d^\omega} && \forall \omega \in \Omega \\
& \psi^{r\omega} = \sum_{i \in \mathcal{R}^\omega} \sum_{j \in \mathcal{R}_i^\omega} \alpha_{i,j}^\omega \hat{y}_{i,j}^{r^\omega} \hat{\pi}_{i,j}^{r^\omega} && \forall \omega \in \Omega \\
& y^{d^\omega} = \sum_{i \in \mathcal{R}^\omega} \sum_{j \in \mathcal{R}_i^\omega} \alpha_{i,j}^\omega \hat{y}_{i,j}^{d^\omega} && \forall \omega \in \Omega \\
& y^{r^\omega} = \sum_{i \in \mathcal{R}^\omega} \sum_{j \in \mathcal{R}_i^\omega} \alpha_{i,j}^\omega \hat{y}_{i,j}^{r^\omega} && \forall \omega \in \Omega \\
& \pi^{d^\omega} = \sum_{i \in \mathcal{R}^\omega} \sum_{j \in \mathcal{R}_i^\omega} \alpha_{i,j}^\omega \hat{\pi}_{i,j}^{d^\omega} && \forall \omega \in \Omega \\
& \pi^{r^\omega} = \sum_{i \in \mathcal{R}^\omega} \sum_{j \in \mathcal{R}_i^\omega} \alpha_{i,j}^\omega \hat{\pi}_{i,j}^{r^\omega} && \forall \omega \in \Omega \\
& \sum_{j \in \mathcal{R}_i^\omega} \alpha_{i,j}^\omega = z_i^\omega && \forall i \in \mathcal{R}^\omega, \forall \omega \in \Omega \\
& \sum_{i \in \mathcal{R}^\omega} z_i^\omega = 1 && \forall \omega \in \Omega \\
& 0 \leq \alpha_{i,j}^\omega \leq 1 && \forall j \in \mathcal{R}_i^\omega, \forall i \in \mathcal{R}^\omega, \forall \omega \in \Omega \\
& z_i^\omega = \{0, 1\} && \forall i \in \mathcal{R}^\omega, \forall \omega \in \Omega
\end{aligned}
$$

Here, y^{d^ω}, $y^{r\omega}$, π^{d^ω} and $\pi^{r\omega}$ are the variables corresponding to strategic consumption, ILR, energy price and reserve price, respectively, for each scenario ω. Also, we define ψ^{d^ω} and $\psi^{r\omega}$ as the

variables corresponding to cost of consumption ($y^{d^\omega}\pi^{d^\omega}$) and revenue of ILR ($y^{r\omega}\pi^{r\omega}$) in scenario ω respectively. In this formulation we use binary variable z_i^ω to determine which region to choose in scenario ω. We call this mathematical program [α-MIP] due to use of α variables that define the convex hull representing each region.

When we solve [α-MIP], optimal values of y^{d^ω}, $y^{r\omega}$, π^{d^ω} and $\pi^{r\omega}$ would form the optimal points corresponding to scenario ω. However, our aim is to calculate two optimal stacks (the consumer's demand-side bid and ILR offer), that are optimal in expectation over all scenarios. In order for the optimal stacks to be admissible to the market, they must be monotone step functions. In particular, the bid stack must be decreasing and the ILR stack increasing. In the next section we probe the issue of monotonicity and its application.

5.1 Monotone Bids

Consider the single scenario case. Here, in the absence of reserve and over a single-node market, the optimal consumption level is effectively singled out by the quantity that determines the dispatch on the (aggregate market) residual supply function. The seminal paper of Klemperer and Meyer [18] lays out the premise for using supply functions as such offers adapt better to uncertain environments faced with multiple scenarios.

It is tempting to determine the optimal quantity of consumption for each scenario, in isolation. The problem with this approach is that the sequence of these consumption decisions may not support a monotone curve. Fig. 10 demonstrates the optimal points obtained by solving [B-L]. Note that there is no single monotone decreasing demand curve that can pass through these 4 points.

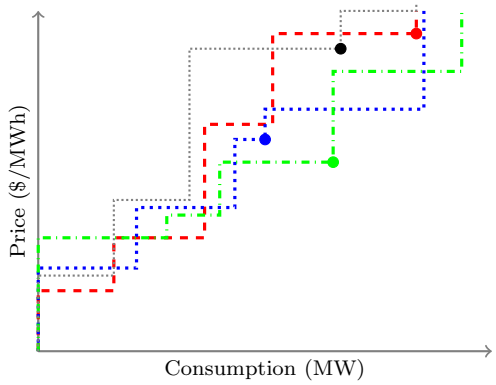

Fig. 10: Optimal wait-and-see bids.

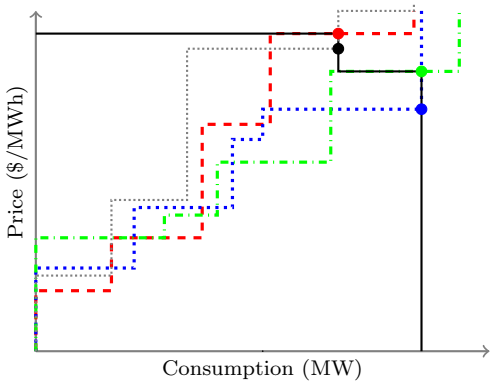

Fig. 11: Optimal monotone consumer bid.

To construct admissible bids, we add monotonicity constraints on the resulting bid and offer curves. To enforce monotonicity, we define binary variables ζ_{ij} to ensure that the energy price in scenario i is higher than that of j provided the quantity consumed in scenario i is less than scenario j. Once the problem is solved with the monotonicity constraints included, we obtain a monotone solution as depicted in Fig. 11.

$$y^{d^i} \leq y^{d^j} + M^d \zeta^d_{i,j} \qquad \forall i,j \in \Omega, i \neq j \tag{5.1}$$

$$y^{r^i} \leq y^{r^j} + M^r \zeta_{i,j} \qquad \forall i,j \in \Omega, i \neq j \tag{5.2}$$

$$\pi^{d^i} \geq \pi^{d^j} - M^\pi \zeta^d_{i,j} \qquad \forall i,j \in \Omega, i \neq j \tag{5.3}$$

$$\pi^{r^i} \leq \pi^{r^j} + M^\pi \zeta^r_{i,j} \qquad \forall i,j \in \Omega, i \neq j \tag{5.4}$$

$$\zeta^d_{i,j} + \zeta^d_{j,i} = 1 \qquad \forall i,j \in \Omega, i \neq j \tag{5.5}$$

$$\zeta^r_{i,j} + \zeta^r_{j,i} = 1 \qquad \forall i,j \in \Omega, i \neq j \tag{5.6}$$

$$\zeta^d_{i,j}, \zeta^r_{i,j} \in \{0,1\} \qquad \forall i,j \in \Omega, i \neq j \tag{5.7}$$

In order to implement the monotonicity constraints to our stochastic models , we add equations (5.1)–(5.7) to [S-MIP]- and [α-MIP]'s constraints. When solving these models with multiple scenarios, the number of constraints and variables increase proportionally with the square of the number of scenarios. In addition, the monotonicity constraints link the scenarios together, meaning that decisions in one scenario may affect the other scenarios' optimal solutions. This yields a large MIP, which can become computationally intractable with a large number of scenarios. Section 6 contains numerical results of implementing our algorithm, and comparison on performances of [S-MIP] and [α-MIP].

6 Numerical Results

In this section we focus on implementing our optimization policies on a major consumer of electricity in New Zealand. The strategic consumer in the case study is the New Zealand Aluminium Smelter (NZAS) which is located in the South Island. We assume the major consumer as a price-maker agent which submits bid and offers to the NZEM's co-optimized OPF that is run every half hour. Whereby, we solve a bi-level optimization problem that maximizes the profit for the major consumer and has the full-scale NZEM's OPF embedded inside, as the lower level problem. In order to solve this bi-level optimization problem, we use the method that we proposed in section 2.

Furthermore, to address uncertainty, we introduce multiple scenarios and optimize the expected profit over a sample set as was discussed in section 5.1. In order to construct the set of scenarios, we use historical data which is publicly available online. We first briefly compare the two proposed stochastic co-optimization models, [S-MIP] and [α-MIP], that we implemented for the NZAS. Table 4 presents the average optimality gap for [S-MIP] and [α-MIP], after one hour of solve time. Similarly, Table 5 compares the number of integer variables in each method, given the sample size. As shown in these tables, the [α-MIP] method has computational advantage and allows us to incorporate larger number of scenarios in our model, hence we use this model for our full-scale NZAS case-study.

Table 4: Average bound gaps (%) versus number of scenarios.

	Number of scenarios									
Method	4	6	8	10	12	14	16	18	20	22
S-MIP	0	12.01	33.61	86.32	-	-	-	-	-	-
α-MIP	0	0	0	0	0	0	0	0	0.8	4.9

Table 5: Number of integers versus number of scenarios.

	Number of scnearios									
Method	4	6	8	10	12	14	16	18	20	22
S-MIP	10504	16961	21078	26388	31710	37048	42350	47648	52988	58360
α-MIP	1101	1838	2392	3342	3744	3991	4677	5237	5924	6332

In order to compute the optimal policies (stacks), we need to choose a sample of scenarios (Ω) from the scenario space. Bid and offer stacks are built to result in here-and-now actions for different types of time-periods, therefore, finding the right combination of scenarios significantly improves the performance of the policies. If we build our scenario set from many similar time-periods that are more likely to happen in the future, we miss the outlier scenarios which could be incorporated

in the bid stack, without altering the optimal response to the more frequent scenarios. Therefore, we avoid picking very similar scenarios in our scenario set (e.g. two consecutive time-periods in one day). This, not only enhances the solve time, by reducing the symmetry in the MIP (and the resulting fractionality), but also enables the major consumer to optimize for various types of time periods, which will form optimal stacks with more tranches. In Appendix C, we provide two examples that develop intuition for sample diversity notation.

We start with simulating our proposed algorithm for the winter peak time-periods. At each iteration of our simulation, in order to define the set Ω, we randomly choose 20 scenarios, from a scenario space consisting of 200 trading-periods from morning peaks, in July and August 2016 and 2017. We construct random sets of Ω, that represent the different types of time periods. 2016 and 2017 are different years in terms of energy prices, and represent a wide range of scenarios. Hence, we have assigned scenarios to 4 different clusters that is based on the average island energy prices in the morning peak trading periods (6 A.M. - 10 A.M.). The sampling scheme is to pick scenarios from all the clusters (i.e. high and low priced weeks), in order to capture the diversity of scenarios.

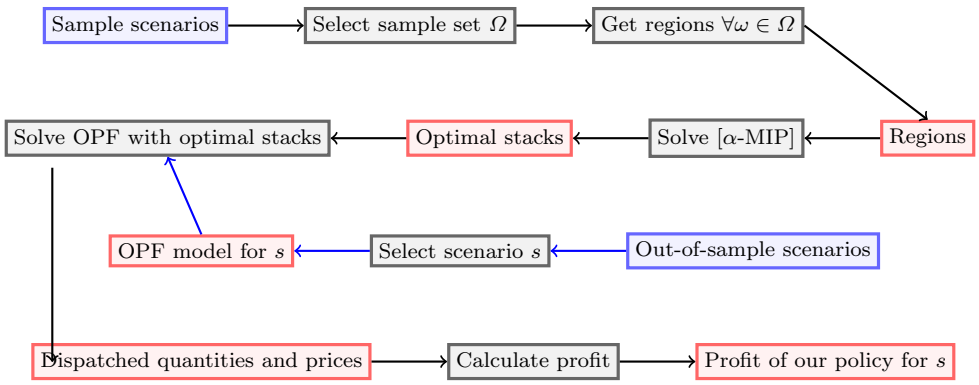

Fig. 12: Optimal Stack Policy Out-of-Sample Simulation Algorithm

After sampling a scenario set, we compute the optimal consumption and ILR stack by solving [α-MIP]. Figure 13 shows the optimal bid stack for the NZAS for one of the sampled scenario sets, that are calculated for different marginal values of consuming electricity (u).

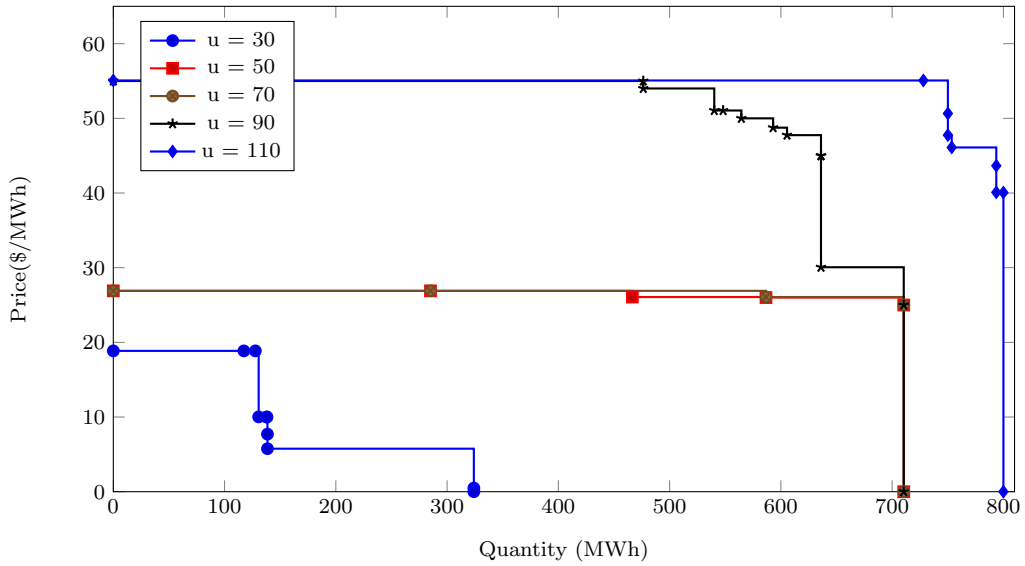

Fig. 13: Optimal Energy Bid Stack - Winter Peak

These optimal stacks need to be submitted to the co-optimized OPF. The aim of this experiment is to test the performance of the optimal stacks that are derived from historical data, and used for the future trading periods. Hence, we simulate our policy for 100 out-of-sample scenarios, and report on the gained profit. Figure 12 outlines the stages of the algorithm in an illustrative diagram.

Finally, we compare our proposed policy with the clairvoyant optimization (absolute upper bound on profit) and the fixed load quantity that is consumed by NZAS in practice. Table 6 outlines the average results of 200 simulations. The experiment is done over different levels of values of electricity (u) to compare the performance of our proposed policy in a broader range parameters. The first column of this table show the average profit over out-of-sample scenarios with our proposed policy's optimal stack. The second column presents the average profit results for the fixed policy in which the consumer targets a fixed quantity. The fixed level is higher for greater u values. The third column reports the average profit of the clairvoyant policy for out-of-sample scenarios. The fourth column shows the increase in profit when using our proposed policy, versus the fixed policy that is now in practice. The last column presents the percentage of clairvoyant policy's profit that is covered by our proposed stochastic out-of-sample policy.

Table 6: Policy Performance- Winter Peak

	Average profit ($)			profit increase	Covering clairvoyant
u	Optimal Stack	Fixed Quantity	Clairvoyant		
30	3405	3245	4313	4.9%	78.9%
50	10209	7283	11004	40.1%	92.7%
70	18474	13438	19783	37.4%	93.3%
90	27238	20006	29655	36.1%	91.8%
110	35993	27529	40895	30.7%	88.0%
Average	19064	14300	21130	29.8%	88.9%

We also simulated policies for off-peak trading periods in winters 2016 and 2017. Table 7 outlines the average results of 300 simulations that implemented the optimal policies for peak and off-peak prices.

Table 7: Winter Policy Performance

	Average profit ($)			profit increase	clairvoyant cover
TP Type	Optimal Stack	Fixed	Clairvoyant		
Winter peak	27238	20006	29655	36.1%	91.8%
Winter off-peak	32395	25343	35301	27.8%	91.7 %

In order to extend the simulation to a broader range of trading periods we have run experiments on 2018/2019 summer which had a series of high prices due to lake levels running low towards the end of summer. We have sampled scenarios from weekdays in December 2017 and January 2018, separately for summer afternoon peak (1 P.M. - 6 P.M.) and early morning off-peak (3 A.M. - 6 A.M.) trading periods. Table 8 outlines the simulation results for summer data.

Note that the sample space of the trading periods have higher price than the same time of year in the previous years. The reason we picked this particular set of trading period is that there had been an anticipation of high prices given the dry summer and low reservoir levels. Hence such signal can be used for major consumers to change their usage plans in order to prevent spike prices. In this experiment we have used a mid February week trading periods as the out-of sample scenarios to show the effect of incorporating our proposed policy while taking into account the anticipation of low lake levels, versus the policy in practice in NZAS which had disregarded the signal.

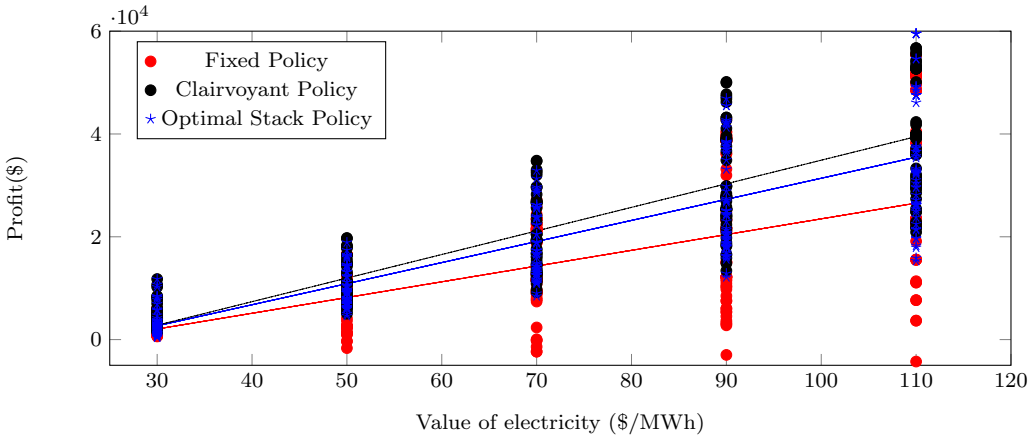

Fig. 14: Winter Peak Profit vs value of electricity u

Table 8: Summer Policy Performance

	Average profit ($)			profit increase	clairvoyant cover
TP Type	Optimal Stack	Fixed	Clairvoyant		
Summer peak	15735	4807	19484	227.3%	80.7%
Summer off-peak	28111	18147	36471	54.9%	77.0 %

7 Conclusions

We addressed major consumers whose demand for energy and ability to provide ILR, affect the market. Our model, given the offers and demand of other market participants, can determine the optimal energy bids and ILR offers for a major consumer. We provided intuition for interactions of demand response and reserve offer decisions. We addressed the uncertainty in energy and reserve markets. Our stochastic model optimizes over a set of scenarios, delivering admissible optimal ILR offer and consumption bid curves for a large consumer of electricity. Using the standard approach requires solving large MIPs due to stochasticity and the resulting monotonicity constraints. In order to reduce the complexity and solve time, we introduced decomposition methods to enhance our formulation. The decomposition has enabled us to apply our method for a major consumer in the NZEM, and solve it over a set of scenarios, consisting of 20 sample time periods, which resulted in around 30% increase in expected profit, compared to a fixed demand policy.

Our model has provided significant intuition for a major consumer's consumption and reserve offer strategy for one trading period. However, a large consumer also can shift consumption of electricity by utilizing flexibility in its production schedule. The consumer's problem, over a sensible time horizon, is the subject of future work.

A Mlti-Node Optimal Power Flow Problem

Here we lay out the OPF problem over a multi-node network. In order to address the network constraints, we use the following notation:

The multi-node dispatch model is laid below. We note this linear program as [M-D-LP].

$$\text{[M-D-LP]} \quad \max_{x^c, x^g} \sum_{t_c \in \mathcal{T}_c} p^c_{t_c} x^c_{t_c} - \sum_{t_g \in \mathcal{T}_g} p^g_{t_g} x^g_{t_g} - \sum_{t_{rg} \in \mathcal{T}_{rg}} p^{rg}_{t_{rg}} x^{rg}_{t_{rg}} - \sum_{t_{rc} \in \mathcal{T}_{rc}} p^{rc}_{t_{rc}} x^{rc}_{t_{rc}}$$

$$\text{s.t.} \quad \sum_{t_c \in \mathcal{T}^n_c} x^c_{t_c} + \sum_{i|ni \in \mathcal{A}} f_{ni} - \sum_{i|in \in \mathcal{A}} f_{in} = \sum_{t_g \in \mathcal{T}^n_g} x^g_{t_g} \qquad [\pi^d_n] \qquad \text{(A.1)}$$

$$- \sum_{n \in \mathcal{N}_e} \sum_{z \in \{rc, rg\}} \sum_{t_z \in \mathcal{T}^n_z} x^z_{t_z} = -r_e \qquad [\pi^r_{e_n}] \qquad \text{(A.2)}$$

f_{ij}	The flow between node i and j.
K_{ij}	The line capacity in arc ij.
r_e	The reserve level required in zone e.
V_n	The minimum amount of difference between ILR and consumption, at node n. It denotes the level of consumption that can not be interrupted.
B_n	The fraction of generation allowed to be offered at reserve, at node n.
W_n	The maximum total amount of generation and reserve, offered by the generator , at node n.
$\mathcal{N}$	The set of all nodes in the network. Note that in our model we have one agent per node. This is not a restrictive assumption.
$\mathcal{A}$	The set of all arcs in the network.
$\mathcal{N}_e$	The set of all nodes in zone e.
L	The loop constraint matrix, where $L_{l,ij}$ corresponds to row l (associated with each loop) and the column ij corresponds to arc ij.
$\mathcal{T'}_c^n$	The set of interruptible consumption tranches.
e_n	indicates the zone that node n is located in.
$\{N, S\}$	The set of islands, north and south.
$\mathcal{Z}$	The set for types of tranches, i.e. consumption, generation, ILR and reserve. $\mathcal{Z} = \{c, g, rc, rg\}$
$\mathcal{T}_z$	The set of all offered tranches of type z.
$\mathcal{T}_z^n$	The set of all tranches of type z at node n
x_t^z	The variable associated with the dispatch quantity tranche type z.
p_t^z	The price of tranche t of type z.
q_t^z	The quantity of tranche t of type z.
[ ]	Variables in [ ] indicate the duals of their associate constraints.

$$\sum_{ij\in\mathcal{A}} L_{l,ij} f_{ij} = 0 \qquad [\lambda_l] \tag{A.3}$$

$$-K_{ij} \le f_{ij} \le K_{ij} \qquad [\eta_{ij}^+, \eta_{ij}^-] \tag{A.4}$$

$$0 \le x_{t_z}^z \le q_{t_z}^z \qquad [\nu_{t_z}^{z+}, \nu_{t_z}^{z-}] \tag{A.5}$$

$$\sum_{t_{rc}\in\mathcal{T}_{rc}^n} x_{t_{rc}}^{rc} - \sum_{t_c\in\mathcal{T'}_c^n} x_{t_c}^c \le 0 \qquad [\theta_n] \tag{A.6}$$

$$\sum_{t_{rg}\in\mathcal{T}_{rg}^n} x_{t_{rg}}^{rg} \le B_n \sum_{t_g\in\mathcal{T}_g^n} x_{t_g}^g \qquad [\phi_n] \tag{A.7}$$

$$\sum_{t_{rg}\in\mathcal{T}_{rg}^n} x_{t_{rg}}^{rg} + \sum_{t_g\in\mathcal{T}_g^n} x_{t_g}^g \le W_n \qquad [\phi'_n]. \tag{A.8}$$

Here (A.1), and (A.6) to (A.8) hold $\forall n \in \mathcal{N}$. (A.2) holds $\forall e \in \{N, S\}$. (A.3) holds for each loop, indicating that sum of impedance adjusted flows across the loop must be zero. (A.4) holds $\forall ij \in \mathcal{A}$. (A.5) holds $\forall t_z \in \mathcal{T}_z, \forall z \in \mathcal{Z}$. Using the OPF model, laid out above, we formulate the bi-level optimization problem, that we call [M-B-L], below:

$$\text{[B-L]} \quad \max_{y^d, y^r} \quad \sum_{n\in\mathcal{N}} \left(u y_n^d - \pi_n^d y_n^d + \pi_{e_n}^r y_n^r \right)$$

$$\text{s.t.} \quad 0 \le y_n^d \le C_n^d \tag{A.9}$$

$$0 \le y_n^r \le C_n^r \tag{A.10}$$

$$y_n^d - y_n^r \ge V_n \tag{A.11}$$

$$\text{[D-LP2]} \quad \max_{x^{z|z\in\mathcal{Z}}} \sum_{t_c\in\mathcal{T}_c} p_{t_c}^c x_{t_c}^c - \sum_{t_g\in\mathcal{T}_g} p_{t_g}^g x_{t_g}^g - \sum_{t_{rg}\in\mathcal{T}_{rg}} p_{t_{rg}}^{rg} x_{t_{rg}}^{rg} - \sum_{t_{rc}\in\mathcal{T}_{rc}} p_{t_{rc}}^{rc} x_{t_{rc}}^{rc}$$

$$\text{s.t.} \quad \text{(A.3)} - \text{(A.8)}$$

$$\sum_{t_c\in\mathcal{T}_c^n} x_{t_c}^c + \sum_{i|ni\in\mathcal{A}} f_{ni} - \sum_{i|in\in\mathcal{A}} f_{in} = \sum_{t_g\in\mathcal{T}_g^n} x_{t_g}^g - y_n^d \qquad [\pi_n^d] \tag{A.12}$$

$$-\sum_{n\in\mathcal{N}_e} \sum_{z\in\{rc,rg\}} \sum_{t_z\in\mathcal{T}_z^n} x_{t_z}^z = \sum_{n\in\mathcal{N}_e} y_n^r - r_e \qquad [\pi_e^r]. \tag{A.13}$$

Here (A.9) to (A.12) hold $\forall n \in \mathcal{N}$, whereas (A.13) holds $\forall e \in \{N, S\}$ (reserve needs are measured and met on the island level).

B Bi-variant Sensitivity Analysis Reformulation Algorithm

Suppose that we have a linear program [LP] in standard computational form:

$$\begin{array}{lll} \text{[LP]} & \min & c^T x \\ & \text{s.t.} & Ax = b \quad [\pi] \\ & & x \geq 0, \end{array}$$

Step 1: Set Initial Values

Set feasible initial values of b_1 and b_2 in [LP]. Without loss of generality, we set $b_1 = b_2 = 0$. Define set $\mathcal{R} = \{\}$ as the set of all regions. Define $\mathcal{R}_r = \{\}$ a subset of $\mathcal{R}$, as the set of all extreme points in region r. Set $r = 1$.

Step 2: Set Initial Optimal Basis

Retrieve the optimal Basis for [LP] given the values of b_1 and b_2. We store the basis data for the vector of basic variables x_B. Note that:

$$\text{Given } Bx_B = b \implies x_B = B^{-1}b \qquad \text{Since } x_B \geq 0 \implies B^{-1}b \geq 0.$$

Step 3: Define [S-LP]

$$\begin{array}{lll} \text{[S-LP]} \max\limits_{b_1, b_2} & c_1 b_1 + c_2 b_2 & \\ \text{s.t.} & B^{-1}_{i,1} b_1 + B^{-1}_{i,2} b_2 \geq 0 & \forall i \in \mathcal{I} \end{array}$$

Here $B^{-1}_{i,1}$ is the first column of the i^{th}row of B matrix, and $\mathcal{I}$ is the set of all rows in B matrix.

Step 4: Set initial c values

At the first iteration we set $c_1 = 1$ and $c_2 = -\infty$.

Step 5: Solve [S-LP]

Solve [S-LP] and add the pair of optimal solution values (b_1^*,b_2^*) to the set $\mathcal{R}_i$.

Step 6: Get objective coefficient sensitivity information

Using sensitivity analysis find largest objective coefficient value (c_2) at which the current optimal basis would remain optimal. Store it as c_2'.

Step 7: Change c_2 coefficient

- If $c_2' \leq \infty$, set $c_2 = c_2' + \epsilon$ in [S-LP] and go to step 5.
- If $c_2' = \infty$ and $c_1 = 1$, go to step 8.
- If $c_2' = \infty$ and $c_1 = -1$, go to step 9.

Step 8: Change c_1 coefficient

Set $c_1 = -1$, and go to step 5.

Step 9: Make seed points

- Define seed set $\mathcal{S} = \{\}$.
- Find the convex hall formed by the pairs in $\mathcal{R}_i$.
- Find an exterior point for each edge, and add the pairs to $\mathcal{S}$ as (b_1^s, b_2^s).
- Set $i = i + 1$

Step 10: Use seed points

- If $\mathcal{S} \neq \emptyset$, choose a pair (b_1^s, b_2^s) from $\mathcal{S}$. Set $b_1 = b_1^s$ and $b_2 = b_2^s$. Remove (b_1^s, b_2^s) from $\mathcal{S}$, and go to step 2.
- if $\mathcal{S} = \emptyset$, go to step 11.

Step 11: Make vertical regions

In order to allow for the optimal solution to lie on the vertical tranches of the residual stack, we add vertical regions to the set of regions $\mathcal{R}$ at this step.

1. Set $i = 1$, and $\mathcal{V} = \{\}$.
2. For each edge in $\mathcal{R}_i$ take the corresponding pairs of (y^d, π_i^d) and (y^r, π_i^r) for the two extreme points on the edge. Store them as point 1 and 2, (e.g. y^{d1}, y^{d2}).
3. Find the adjacent region j to the chosen edge, and store π_j^d and π_j^r.
4. Set $\mathcal{Q} = \{\{(y^{d1}, \pi_i^d), (y^{r1}, \pi_i^r)\}, \{(y^{d2}, \pi_i^d), (y^{r2}, \pi_i^r)\}, \{(y^{d1}, \pi_j^d), (y^{r1}, \pi_j^r)\}, \{(y^{d2}, \pi_j^d), (y^{r2}, \pi_j^r)\}\}$.
5. If $\mathcal{Q} \notin \mathcal{V}$, add $\mathcal{Q}$ to $\mathcal{V}$.
6. Set $i = i + 1$
7. If $i \leq |\mathcal{R}|$, go back to line 2.
8. If If $i = |\mathcal{R}|$, set $\mathcal{R} = \mathcal{R} \cup \mathcal{V}$

C Scenario Selection Examples

Here we propose an example to illustrate our choice of a scenario set regarding the similarity of scenarios. In this example we use the full-scale network's historical data. Suppose, $|\Omega_1| = |\Omega_2| = 6$ are two scenarios sets. Here Ω_1 consists of similar scenarios, all picked from a morning peak on a single day, in winter 2016. In addition, Ω_2 consists of semi-similar scenarios, chosen from morning peaks of two days in winter 2016 and 2017. We solve [α-MIP] for both sets and obtain the optimal expected actions for each scenario set. Figure 15 shows the optimal stacks the two sample sets, here S1 and S2 correspond to optimal bid stacks from optimizing against Ω_1 and Ω_2 respectively.

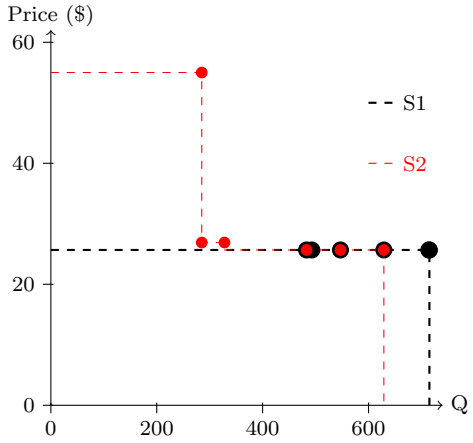

Fig. 15: Sample set comparison

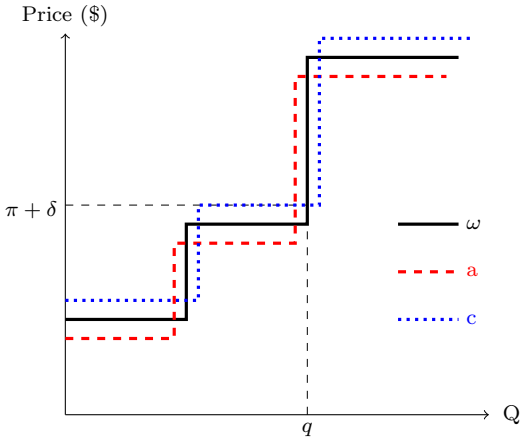

Fig. 16: Similar Scenarios

As shown in figure 15, S2 consists of three steps, which enables it to respond to different types of time periods. The three mutual scenarios in the two scenarios sets, have the same optimal consumption - price pairs in the two stacks (the overlapped points), which results in equal in-sample profit for the mutual points. In addition, the diversity of scenarios in Ω_2, S2 enhance its performance for out-of-sample scenarios. Table 9 report on each stack's profit when simulated for 100 scenarios.

Table 9: Out-of-Sample Performance Comparison

	Profit ($)		
Stack	Average	Min.	Max.
S1	15707	10109	21571
S2	17841	12238	21637

Here, we use a generic example to parametrically calculate the impact of scenario selection. Suppose we have scenario ω, with the residual supply stack shown with black line in Figure 16, with the optimal consumption-price pair (q, π). We introduce new scenarios (a – d), whose residual stack deviates from that of ω with distance δ in each dimension. For the sake of simplicity we only show 2 out of 4 stacks (a and c) in Fig. 16. Here scenario a's residual

stack is shown in red, and its optimal consumption-price pair is $(q-\delta, \pi-\delta)$, and that of scenario c is $(q+\delta, \pi+\delta)$. Similarly, scenario b and d have the optimal consumption-price pairs $(q-\delta, \pi+\delta)$ and $(q+\delta, \pi-\delta)$, respectively. If we solve [α-MIP] for $\Omega = \{\omega\}$, the optimal stack will have one step with the point (q, π). However, in order to cover the optimal consumption for the scenarios whose prices are higher with $\$\delta$ divergence from π, we draw the optimal stack based on the quantity-price pair $(q, \pi+\delta)$, which is presented with the dashed gray line in Figure 16. We call this stack ω-stack.

In table 10 we compare using the clairvoyant policy versus the optimal stack generated with Ω, for all scenarios ω and a–d. Here the difference between the clairvoyant policy and ω-stack, depends on δ. Note that when we set $\delta << q$, the difference in profit becomes very small, and it would be beneficial to pick a representative scenario in Ω, instead of including all similar scenarios.

Table 10: Profit vs Policy

Scenario	Clairvoyant	ω-stack	Difference
ω	$(u-\pi)q$	$(u-\pi-\delta)q$	δq
a	$(u-\pi+\delta)(q-\delta)$	$(u-\pi-\delta)(q-\delta)$	$2\delta(q-\delta)$
b	$(u-\pi-\delta)(q-\delta)$	$(u-\pi-\delta)(q-\delta)$	0
c	$(u-\pi-\delta)(q+\delta)$	$(u-\pi-\delta)q$	$\delta(u-\pi-\delta)$
d	$(u-\pi+\delta)(q+\delta)$	$(u-\pi+\delta)q$	$\delta(u-\pi+\delta)$

The example above shows that the more scenarios are similar to one another, the less the objective function will improve by including them in the optimal bid stack. Hence, we construct our random sets Ω, while ensuring two similar scenarios are not picked. However, the information on the number of occurrences of similar scenarios will be incorporated in the probability of the representative scenario.

References

1. M. H. Albadi and E. El-Saadany, *A summary of demand response in electricity markets*, Electric power systems research, 78 (2008), pp. 1989–1996.
2. A. G. Bakirtzis, N. P. Ziogos, A. C. Tellidou, and G. A. Bakirtzis, *Electricity producer offering strategies in day-ahead energy market with step-wise offers*, IEEE Transactions on Power Systems, 22 (2007), pp. 1804–1818.
3. K. Bhattacharya et al., *Competitive framework for procurement of interruptible load services*, IEEE Transactions on Power systems, 18 (2003), pp. 889–897.
4. D. W. Caves and J. A. Herriges, *Optimal dispatch of interruptible and curtailable service options*, Operations Research, 40 (1992), pp. 104–112.
5. N. Cleland, G. Zakeri, G. Pritchard, and B. Young, *Boomer-consumer: a model for load consumption and reserve offers in reserve constrained electricity markets*, Computational Management Science, 12 (2015), pp. 519–537.
6. N. Cleland, G. Zakeri, G. Pritchard, and B. Young, *Integrating consumption and reserve strategies for large consumers in electricity markets*, in Computational Management Science, Springer, 2016, pp. 23–30.
7. A. J. Conejo, J. Contreras, J. M. Arroyo, and S. De la Torre, *Optimal response of an oligopolistic generating company to a competitive pool-based electric power market*, Power Systems, IEEE Transactions on, 17 (2002), pp. 424–430.
8. P. Cramton and S. Stoft, *A capacity market that makes sense*, The Electricity Journal, 18 (2005), pp. 43–54.
9. A. Daraeepour, S. J. Kazempour, D. Patiño-Echeverri, and A. J. Conejo, *Strategic demand-side response to wind power integration*, IEEE Transactions on Power Systems, 31 (2016), pp. 3495–3505.
10. E. Ela, M. Milligan, and B. Kirby, *Operating reserves and variable generation*, Contract, 303 (2011), pp. 275–3000.
11. J. F. Ellison, L. S. Tesfatsion, V. W. Loose, and R. H. Byrne, *Project report: A survey of operating reserve markets in us iso/rto-managed electric energy regions*, Sandia Natl Labs Publications. Available Online: http://www. sandia. gov/ess/publications/SAND2012, 1000 (2012).
12. J. Fortuny-Amat and B. McCarl, *A representation and economic interpretation of a two-level programming problem*, Journal of the operational Research Society, (1981), pp. 783–792.
13. B. F. Hobbs, C. B. Metzler, and J.-S. Pang, *Strategic gaming analysis for electric power systems: An mpec approach*, IEEE transactions on power systems, 15 (2000), pp. 638–645.
14. S. J. Kazempour, A. J. Conejo, and C. Ruiz, *Strategic bidding for a large consumer*, IEEE Transactions on Power Systems, 30 (2015), pp. 848–856.
15. D. S. Kirschen, *Demand-side view of electricity markets*, IEEE Transactions on Power Systems, 18 (2003), pp. 520–527.
16. N. Li, L. Chen, and S. H. Low, *Optimal demand response based on utility maximization in power networks*, in Power and Energy Society General Meeting, 2011 IEEE, IEEE, 2011, pp. 1–8.
17. S. Majumdar, D. Chattopadhyay, and J. Parikh, *Interruptible load management using optimal power flow analysis*, IEEE Transactions on Power Systems, 11 (1996), pp. 715–720.
18. M. A. M. Paul D. Klemperer, *Supply function equilibria in oligopoly under uncertainty*, Econometrica, 57 (1989), pp. 1243–1277, `http://www.jstor.org/stable/1913707`.

19. M. V. Pereira, S. Granville, M. H. Fampa, R. Dix, and L. A. Barroso, *Strategic bidding under uncertainty: a binary expansion approach*, IEEE Transactions on Power Systems, 20 (2005), pp. 180–188.
20. C. Ruiz and A. J. Conejo, *Pool strategy of a producer with endogenous formation of locational marginal prices*, IEEE Transactions on Power Systems, 24 (2009), pp. 1855–1866.
21. H. Sæle and O. S. Grande, *Demand response from household customers: experiences from a pilot study in norway*, Smart Grid, IEEE Transactions on, 2 (2011), pp. 102–109.
22. F. C. Schweppe, R. D. Tabors, M. Caraminis, and R. E. Bohn, *Spot pricing of electricity*, (1988).
23. C.-L. Su and D. Kirschen, *Quantifying the effect of demand response on electricity markets*, IEEE Transactions on Power Systems, 24 (2009), pp. 1199–1207.
24. K. M. Tsui and S.-C. Chan, *Demand response optimization for smart home scheduling under real-time pricing*, Smart Grid, IEEE Transactions on, 3 (2012), pp. 1812–1821.